Am J Transl Res 2016;8(2):365-374
www.ajtr.org /ISSN:1943-8141/AJTR0014484

Original Article

Nerve distribution of canine pulmonary arteries and potential clinical implications

Yun Zhang[1], Weijie Chen[1], Yanping Xu[1], Hang Liu[1], Yunlin Chen[1], Hanxuan Yang[1], Yuehui Yin[2]

[1]Department of Cardiology, The Second Affiliated Hospital of Chongqing Medical University, 76 Linjiang Road, Yuzhong District, Chongqing, 400010, China; [2]Department of Cardiology, Chongqing Cardiac Arrhythmias Therapeutic Service Center, The Second Affiliated Hospital of Chongqing Medical University, 76 Linjiang Road, Yuzhong District, Chongqing, 400010, China

Received August 13, 2015; Accepted December 24, 2015; Epub February 15, 2016; Published February 29, 2016

Abstract: Sympathetic activation plays an important pathophysiological role in the progression of pulmonary artery hypertension. Although adrenergic vasomotor fibers are present in the adventitia of pulmonary arteries, the anatomy of the peri-arterial pulmonary nerves is still poorly understood. The aim of the current study was to determine the sympathetic nerve distribution in canine pulmonary arteries. A total of 2160 sympathetic nerves were identified in six Chinese Kunming canines. Nerve counts were greatest in the proximal segment, with a slight decrease in the distal segment; the middle segment showed the least number of nerves. In the left and right pulmonary arteries, 77.61% and 78.97% of the nerves were located within a 1-3-mm range, respectively. The number of nerves in the posterior region of the bifurcation and pulmonary trunk outnumbered those in the anterior region. Furthermore, 65.33% of the nerves were located in the first 2-mm range of the posterior region of bifurcation, and 89.62% of the nerves were located within the 1-3-mm range of the posterior region of the pulmonary trunk. In conclusion, a great abundance of sympathetic nerves occurred in the proximal and distal segments of the bilateral pulmonary arteries. There is a clear predominance of sympathetic nerve distribution in the posterior region of the bifurcation and pulmonary trunk. This anatomic distribution may have implications for the future development of percutaneous pulmonary artery denervation.

Keywords: Bifurcation of the pulmonary trunk, pulmonary trunk, sympathetic, pulmonary artery, percutaneous pulmonary artery denervation

Introduction

Pulmonary artery hypertension (PAH) is a complex vascular remodeling disease [1], characterized by medium-sized and small pulmonary arteries with medial and adventitial hypertrophy and intimal proliferative changes [2, 3]. It contributes to increased pulmonary vascular resistance, leading to heart failure and death [4]. PAH is multifactorial: It is unlikely that one factor or gene mutation can explain all forms of PAH [5]. The currently approved therapies neither improve survival nor reverse the progression of the disease. Moreover, current therapies lack specificity for pulmonary vessels, as all of these therapies originated for the treatment of systemic vascular disease [1]. The overall effect of the current therapies on hemodynamics and functional capacity is minimal, and thus new therapeutic strategies are urgently needed in the near future [6]. Velez-Roa et al. [7] reported an increase in sympathetic nerve activity in patients with PAH, potentially promoting the progression of PAH. Recently, the First-in-Man PADN-1 study showed that percutaneous pulmonary artery denervation (PADN) could reduce pulmonary artery pressure (PAP) and pulmonary vascular resistance (PVR) due to injury to the main pulmonary artery bifurcation area, improving cardiac function and functional capacity of patients with idiopathic PAH [8]. It has been realized that sympathetic activation may participate in pulmonary arteriolar remodeling. The aim of the present study was to examine the anatomic characteristics of canine pulmonary artery nerves with respect to density, size, and distance from the pulmonary artery lumen intima, and to discuss the potential therapeutic targets for PADN.

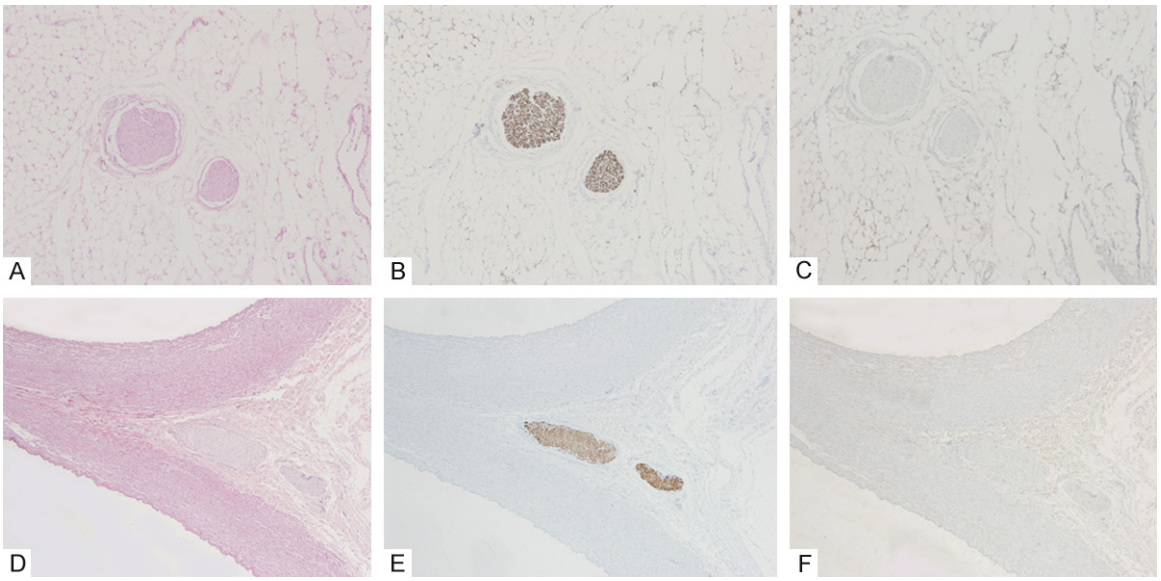

Figure 1. Immunohistochemistry of sympathetic vs. vagus nerve fibers. A, D. Hematoxylin and eosin staining. B, E. Strong staining of tyrosine hydroxylase. C, F. Negative expression of choline acetyltransferase. A-F. Original magnification×40.

Materials and methods

Experimental design

The study was approved by the animal experimentation ethics committee of Chongqing Medical University, following the guidelines of the National Institutes of Health for the care and use of laboratory animals. In total, six Chinese Kunming male canines, 3 to 3.5 years of age and weighing 30 to 35 kg, were used in this study. To obtain tissues for the study, after the canines were anesthetized with 3% sodium pentobarbital by intraperitoneal injection, the thoracic cavity was opened, and the bilateral lung, heart, trachea, and the surrounding tissues were exposed. The right ventricle, pulmonary trunk, bifurcation of the pulmonary trunk, and the bilateral pulmonary arteries were then exposed, extracted, and perfusion/fixed ex vivo under physiological pressure (80 to 100 mm Hg) with 10% neutral buffered formalin. The anterior region of the pulmonary trunk and the bifurcation of the pulmonary trunk were tagged with red tagging. Correspondingly, the other side is the posterior region of the pulmonary trunk and the bifurcation. A total of 48 segments, including the pulmonary trunk, bifurcation of the pulmonary trunk, and the equal proximal, middle, and distal segments of the left and right pulmonary arteries were collected from six canines.

Histopathology and immunohistochemistry

A total of 36 pulmonary artery segments, six bifurcations of the pulmonary trunks, and six pulmonary trunks were fixed by immersion in 4% paraformaldehyde in phosphate-buffered saline. Each paraffin-embedded specimen with surrounding soft tissue was sectioned at 1-mm intervals, producing three to five segments. Every segment was cut into five serial sections at a thickness of 5 μm and stained with hematoxylin and eosin, tyrosine hydroxylase (TH) [9], and choline acetyltransferase (ChAT) for sympathetic and vagus nerve fibers [10], and neurofilament protein (NFP) for nerve size measurements [11].

Paraffin-embedded slides were de-paraffinized and hydrated. For antigen retrieval, sections were boiled under pressure in EDTA for 10 minutes. After rinsing, the sections were incubated with rabbit polyclonal anti-TH (1:200; Abcam, Cambridge, UK) and rabbit polyclonal anti-ChAT (1:400; Abcam), and mouse monoclonal anti-neurofilament heavy antibody (1:100; Abcam) overnight at 4°C. Slides were then incubated with a species-specific biotinylated secondary antibody for 30 minutes at 30°C. Detection was performed using DAB (ZSGB-BIO, Beijing, China). The resulting slides were examined via light microscopy and analyzed with Image-Pro Plus software (Windows version 6.0 Media Cybernetics, Rockville, MD).

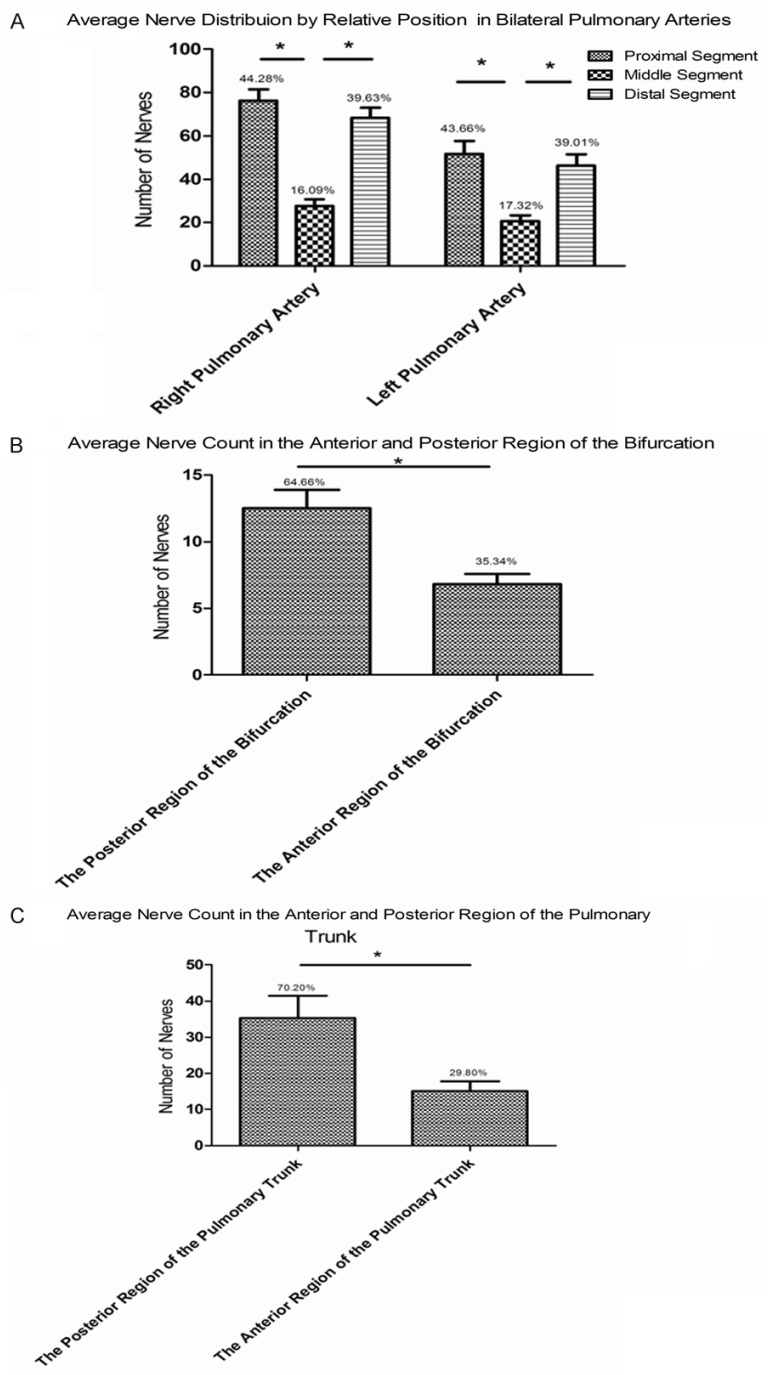

Figure 2. Nerve counts. A. Compared with the middle segment, the number of nerves in the proximal and distal segments was greater. *p<0.01. B. The average nerve count in the posterior region was greater than that in the anterior region of the bifurcation. *p<0.05. C. The average nerve count in the posterior region was greater than that in the anterior region of the pulmonary trunk. *p<0.01.

Statistical analysis

Morphometric analysis was conducted on the digital scans using Image-Pro Plus software to quantify the following parameters: number of nerves per section (nerve count), distance of all counted objects (nerves) to the lumen intima of the vessel, and the diameter of all counted objects. Nerve counts were summed for each arterial segment (proximal, middle, distal, anterior, and posterior regions of the bifurcation, and anterior and posterior regions of the pulmonary trunk) based on individual artery lengths. The nerve's smallest diameter was used to calculate a theoretical sectional area correcting for the frequent oblique sectioning of the nerves, as a best estimate of nerve diameter. Experimental values are expressed as the mean ± SD. The Shapiro-Wilk test was used to statistically assess violations of the normal distribution assumption. For statistical comparison of the nerve distribution, mean values of nerve counts were derived for proximal, middle, and distal regions, as well as for the posterior and anterior regions of the bifurcation and pulmonary trunk, and analyzed using paired Student's *t* tests. For skewed data distribution, a matched comparison using the Wilcoxon signed rank or Friedman test was applied. All of the statistical analyses were performed with SPSS statistical software (version 18.0, Chicago, Illinois, USA). A two-sided *p* value less than <0.05 was regarded as statistically significant.

Results

Immunohistochemistry

Immunohistochemical staining indicated the presence of TH positive sympathetic fibers in the adventitial layer of the pulmonary artery, bifurcation, and pulmonary trunk; however,

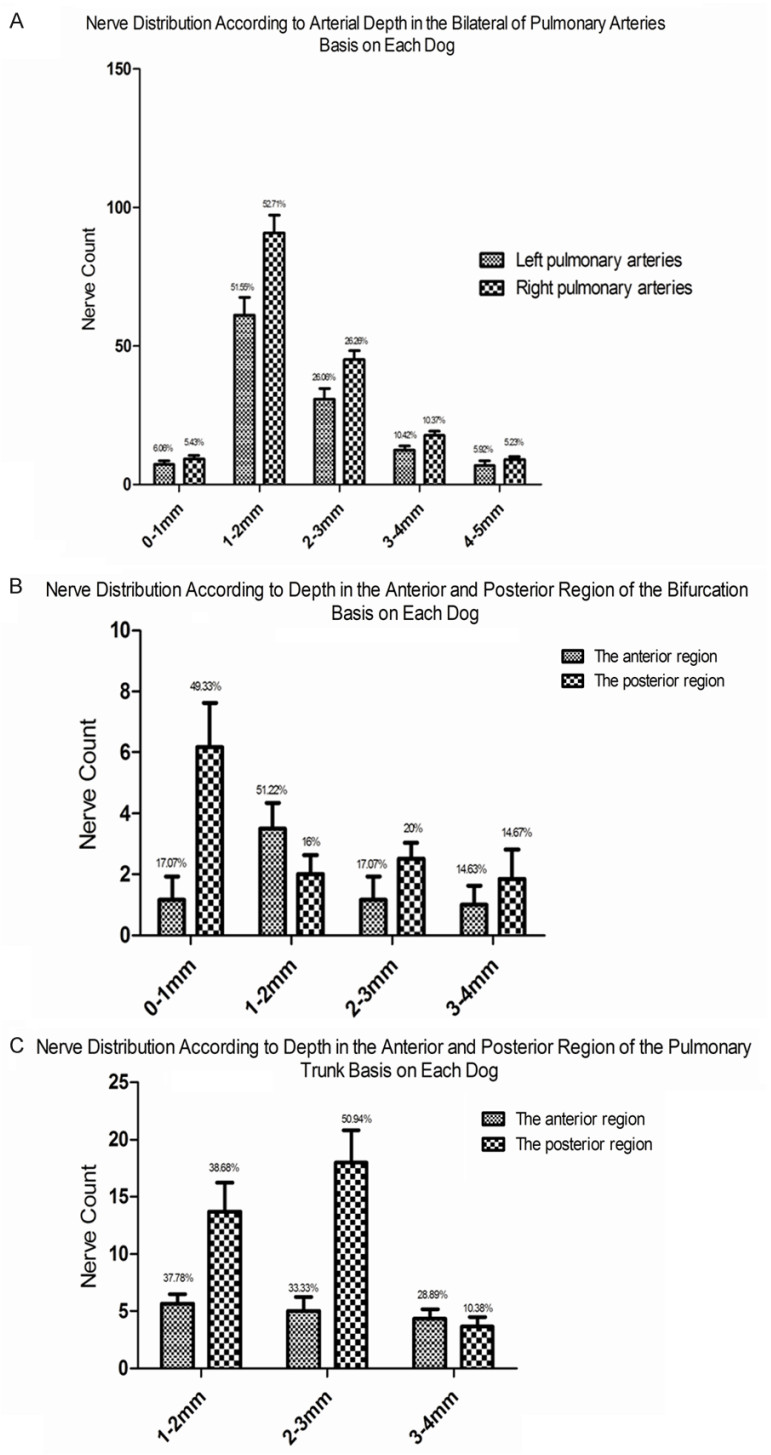

Figure 3. Nerve distribution by depth. A. Average nerve distribution between 0 and 5 mm in the bilateral pulmonary arteries. B. Average nerve distribution between 0 and 4 mm in the anterior and posterior regions of the bifurcation. C. Average nerve distribution between 0 and 4 mm in the anterior and posterior regions of the pulmonary trunk.

there were no ChAT-positive vagus fibers (**Figure 1**).

Nerve count

The nerve distribution patterns were similar between the left and right pulmonary arteries, but the average number of nerves located in the right pulmonary artery was greater than that in the left pulmonary artery. Categorizing the nerves in the proximal, middle, and distal segments of the pulmonary artery, the proximal and distal segments displayed comparable nerve counts, whereas the middle segment had the fewest nerves (**Figure 2A**). In the right pulmonary artery, 44.28% (76.17 ± 5.31) of the nerves were seen in the proximal segment, with a slight decrease in the distal segment (39.63%, 68.17 ± 4.88), and the lowest number of nerves was located in the middle segment (16.09%, 27.67 ± 3.01). The numbers of nerves in the proximal and distal segments of the left pulmonary artery were 43.66% (51.67 ± 6.06) and 39.01% (46.17 ± 5.38), respectively, whereas 17.32% (20.5 ± 2.81) of nerves were found in the middle segment.

There were more nerves in the posterior region (64.66%, 12.5 ± 1.38) of the bifurcation of the pulmonary artery than in the anterior region (35.34%, 6.83 ± 0.75) (**Figure 2B**). Similarly, the average number of nerves in the posterior region of the pulmonary trunk (70.20%, 35.33 ± 6.09) was greater than that (29.80%, 15 ± 2.76) in the anterior region (**Figure 2C**).

Nerve distribution by depth

From all cross-sections, a significant proportion of nerves was identified in the 1-3-mm range

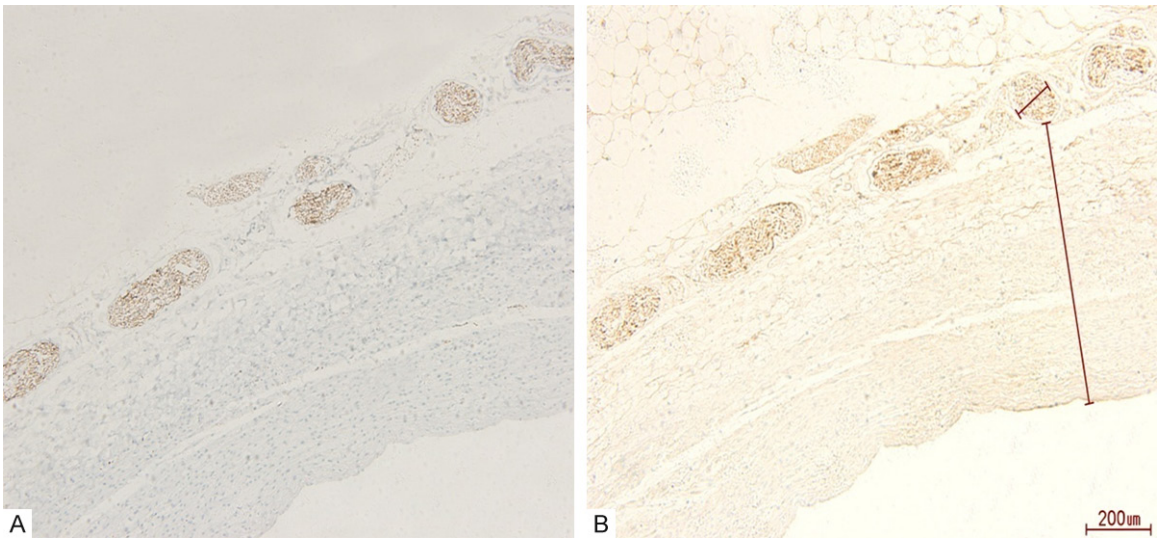

Figure 4. The correlation between the number of nerves identified using tyrosine hydroxylase and neurofilament protein staining. A. Tyrosine hydroxylase stain (TH). B. Neurofilament protein (NFP) stain. A and B. Original magnification×100.

away from the lumen intima of the right (78.97%, 135.83 ± 9.72) and left (77.61%, 91.83 ± 10.11) pulmonary artery (**Figure 3A**). According to the distance from the nerve to the bifurcation of the pulmonary trunk, there was a high innervation in the 0-2-mm range in the posterior region (65.33%, 8.17 ± 2.1), and more than 50% of nerves existed within the 1-3-mm range in the anterior region (68.29%, 4.67 ± 1.59) (**Figure 3B**). A total of 71.11% (10.67 ± 2.08) and 89.62% (31.67 ± 5.41) of nerves were found in the 1-3-mm range of the pulmonary trunk in both the anterior and posterior regions (**Figure 3C**). Furthermore, in the posterior region of the pulmonary trunk, 50.94% (18 ± 2.83) of nerves were located in the 2-3-mm range (**Figure 3C**).

Nerve distribution by size

The number of nerves identified by NFP and TH immunohistochemical staining correlated well (**Figure 4**). The nerve distribution by size was similar between the left and right pulmonary arteries (**Figure 5A**). More than 50% of the nerves were between 100-300 μm in diameter: 68.31% (80.83 ± 8.77) of them were in the left pulmonary artery and 69.38% (119.34 ± 8.35) were in the right pulmonary artery. In the left pulmonary artery, 25.63% (30.33 ± 4.13) of the nerves were between 300 μm to 400 μm in diameter, whereas 6.06% (7.17 ± 1.33) were between 0 and 100 μm in diameter. In the right pulmonary artery, 25.19% (43.33 ± 3.50) of the nerves were between 300 μm and 400 μm in diameter, whereas 5.43% (9.33 ± 1.21) were between 0 and 100 μm in diameter.

Categorizing the nerves in the proximal, middle, and distal pulmonary artery segments, the nerve distribution pattern was different in each segment (**Figure 5B** and **5C**). In the proximal segment of the left pulmonary artery, 86.45% (44.66 ± 4.82) of the nerves were between 100 μm and 300 μm in diameter, of which 53.87% (27.83 ± 2.99) were between 100 μm and 200 μm in diameter, with only 8.39% (4.33 ± 1.03) between 300 μm and 400 μm in diameter. In the distal left pulmonary artery segment, the majority of nerves were between 300 μm and 400 μm in diameter (48.74%, 22.5 ± 2.59), 5.78% (2.67 ± 0.52) were less than 100 μm in diameter, and 45.49% (21 ± 2.45) were between 100 μm to 300 μm in diameter (100-200 μm, 24.91%, 11.5 ± 1.22; 200-300 μm, 20.58%, 9.5 ± 1.22). In the three segments of the right pulmonary artery, the size distribution pattern was similar to that in the left, and the distal segment demonstrated a higher proportion of nerves of a larger size (300-400 μm, 49.14%, 33. 5 ± 2.59); conversely, the proximal segment showed a significant proportion of nerves of a smaller size (0-100 μm, 5.03%, 3.83 ± 0.75; 100-200 μm, 54.27%, 41.33 ± 2.73).

Nerve size was significantly different between the anterior and posterior regions of the bifur-

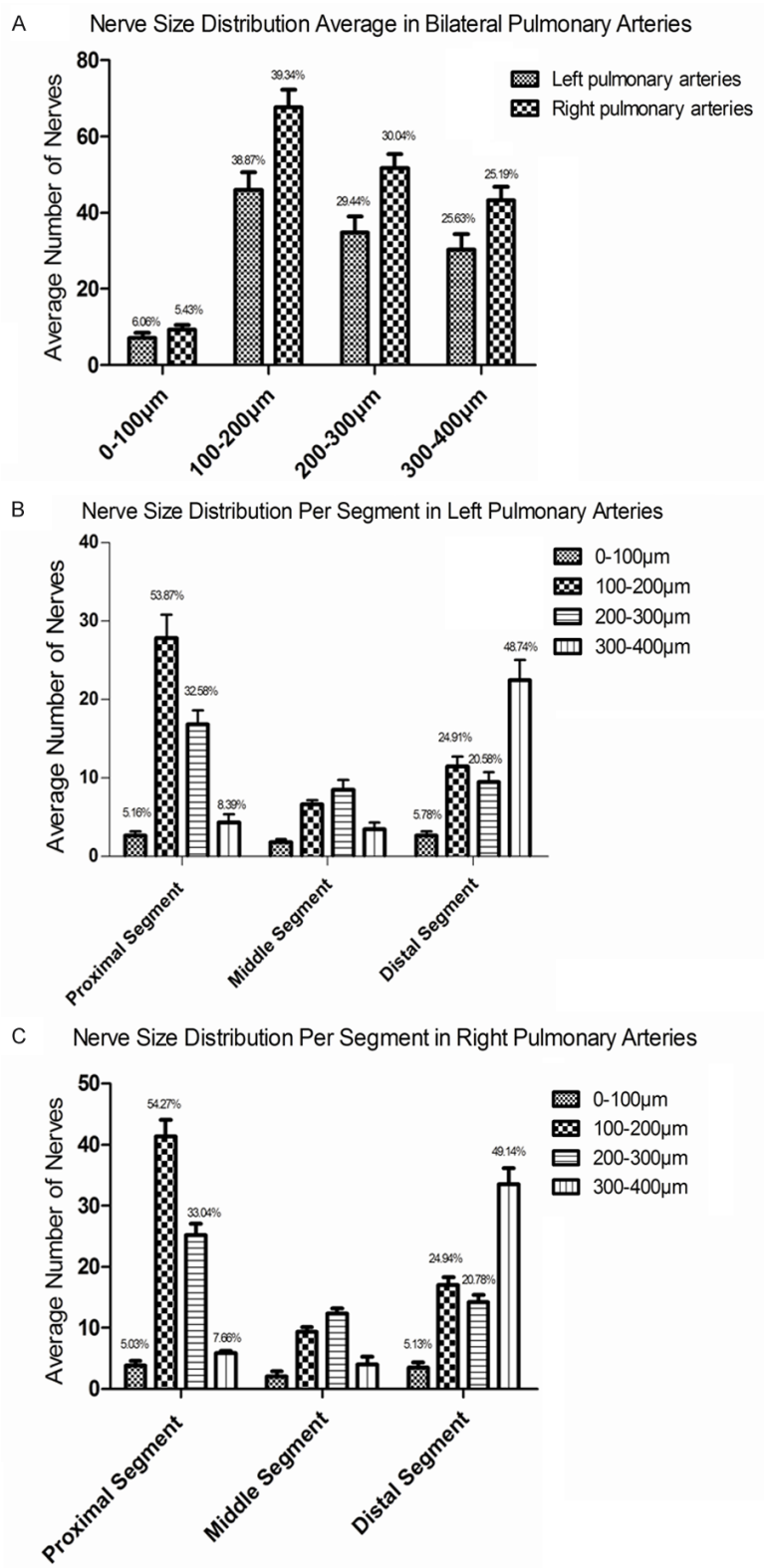

Figure 5. Nerve size of the bilateral pulmonary arteries. A. More than 50% of the nerves were between 100-300 μm. B. In the proximal segment, 53.87% of nerves were between 100-200 μm, and 48.74% nerves were between 300-400 μm in the distal segment. C. In the proximal segment, 54.27% nerves were between 100-200 μm, and 49.14% of nerves were between 300-400 μm in the distal segment.

cation of the pulmonary trunk (**Figure 6A**). In the anterior region, the number of smaller nerves was greater than the number of larger nerves: 70.73% (4.84 ± 0.93) were 100-300 μm size in diameter, 12.20% (0.83 ± 0.41) were 300-400 μm in diameter, and 17.07% (1.17 ± 0.41) were 400-500 μm in diameter. In the posterior region, the majority of nerves were larger: 18.67% (2.33 ± 0.52) were 300-400 μm in diameter, 49.33% (6.17 ± 1.17) were 400-500 μm in diameter, 20% (2.5 ± 0.84) were 200-300 μm in diameter, and only 12% (1.5 ± 0.55) were 100-200 μm in diameter. The nerves in the posterior region of the pulmonary trunk tended to be larger: 40.57% (14.33 ± 2.07) were 500-600 μm in diameter, 24.53% (8.67 ± 1.51) were 600-700 μm in diameter, and 34.91% (12.33 ± 3.05) were 100-500 μm in diameter. In the anterior region of the pulmonary trunk, the nerve distribution became relatively equal across all sizes (100-200 μm, 8.89%, 1.33 ± 0.52; 200-300 μm, 16.67%, 2.5 ± 0.55; 300-400 μm, 28.89%, 4.33 ± 0.82; 400-500 μm, 21.11%, 3.17 ± 0.41; 500-600 μm, 16.67%, 2.5 ± 0.55; and 600-700 μm, 7.78%, 1.17 ± 0.41) (**Figure 6B**).

Discussion

In the present study, we examined the anatomical distribution of peri-arterial sympathetic nerves around canine pulmonary arteries. We analyzed the nerve distribution in the left and right pulmonary arteries up to a 5-mm depth from the lumen intima, 4 mm of the peripheral tissue

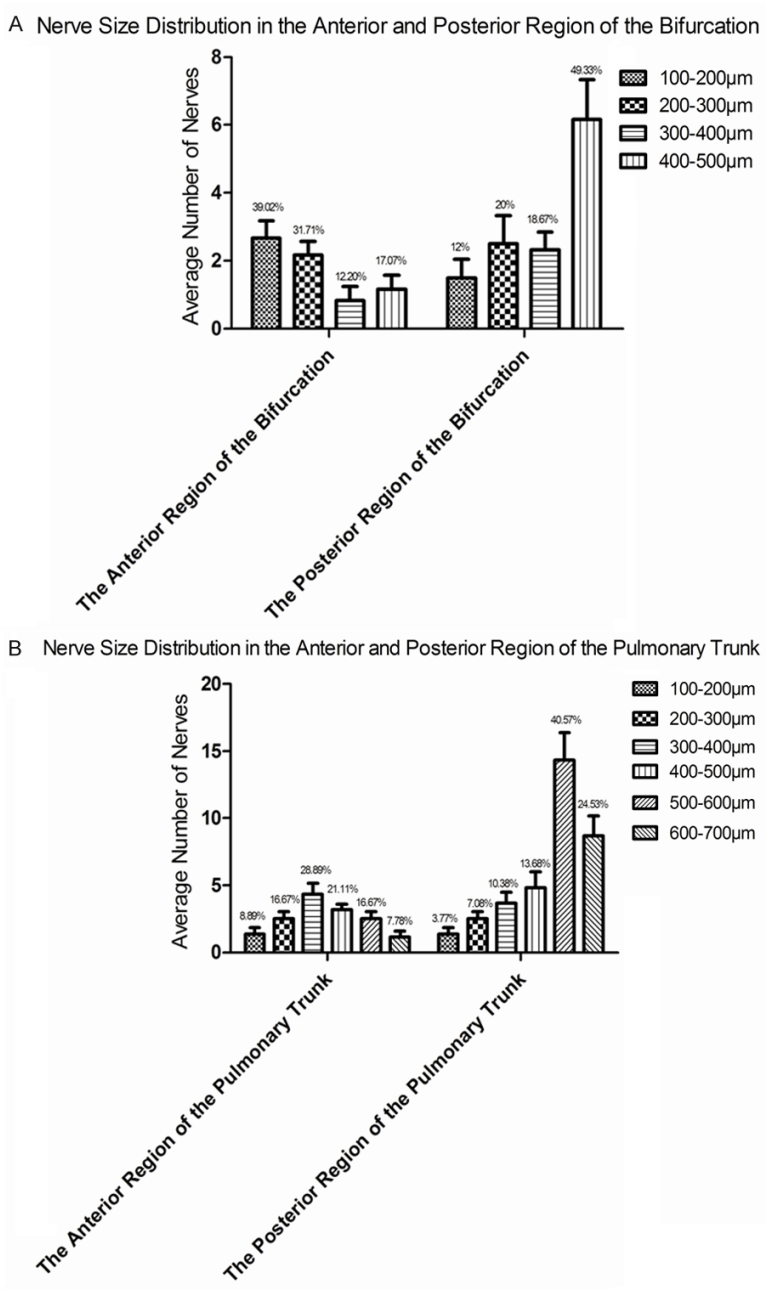

Figure 6. Nerve size of the bifurcation and pulmonary trunk. A. In the posterior region of the bifurcation, 49.33% nerves were between 400-500 μm in diameter. B. In the posterior region of the pulmonary trunk, 65.10% nerves were between 500-700 μm in diameter.

around the pulmonary trunk intima, and the anterior and posterior regions up to a distance of 4 mm from the pulmonary arterial bifurcation. Interestingly, we only found TH-positive fibers, but no ChAT-positive fibers. Compared with the middle segments, the quantities of sympathetic nerves were higher in the proximal and distal segments of the bilateral pulmonary artery: 77.61% and 78.97% of nerves were distributed within a 1-3-mm range from the lumen intima of the left and right pulmonary arteries, respectively. The total quantity of nerves in the posterior region of the bifurcation and the pulmonary trunk was greater than that in the anterior region: 49.33% of nerves were located at a depth of 1 mm away from the bifurcation in the posterior region of the bifurcation, and 50.94% were at a depth range of 2-3-mm away from the pulmonary trunk in the posterior region of the pulmonary trunk.

An increasing number of studies have showed that sympathetic nerve activity increases in PAH, with the severity and prognosis of PAH correlated to sympathetic nerve activity [12-14]. Although current PAH therapy focuses on reversing the imbalance between vasoconstrictors and vasodilators, it does not significantly improve survival [6]. Furthermore, the activities of sympathetic nerves vary with disease conditions [7]. It would follow to question whether it might be possible to delay the progression of the pathophysiological state of PAH by removing the nerves of the pulmonary arteries. A recent study reported that the mean PAP of 21 idiopathic PAH patients was improved following PADN at the main bifurcation area of the pulmonary artery [8]. Thus, gaining knowledge of the anatomic distribution of the sympathetic nerves may help the development of pulmonary denervation therapies.

In our study, we examined up to 5 mm of the peripheral tissue around the pulmonary artery, and up to 4 mm around the bifurcation and pul-

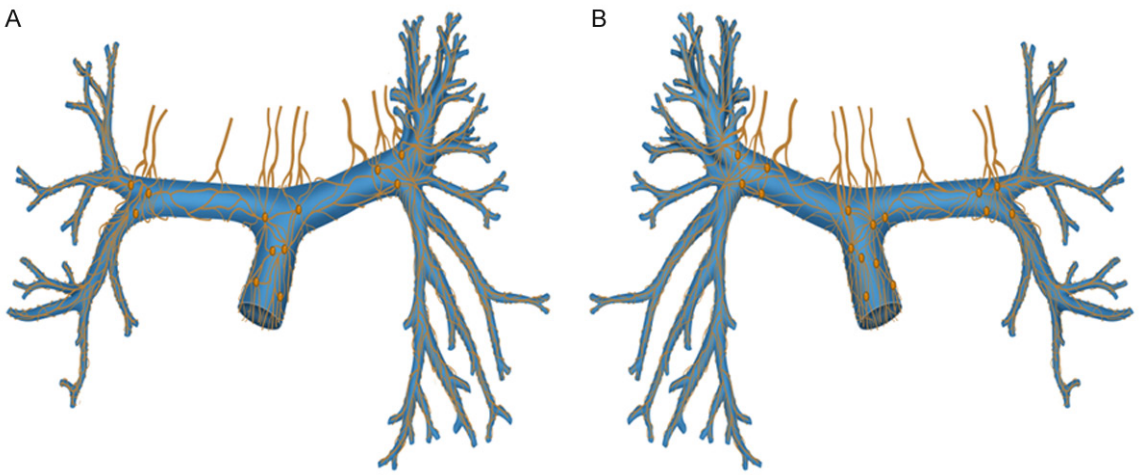

Figure 7. Thermal energy could be focused on the posterior region of the bifurcation and pulmonary trunk, as well as on the initial portions and roots of the right and left pulmonary artery. A. Anterior. B. Posterior.

monary trunk; we did not identify any vagus nerves. One explanation for this phenomenon is that the pulmonary artery may not be a neuro-effector organ of the vagus nerves, as postsynaptic sympathetic fibers primarily function to innervate all of the body's vessels [15]. This explanation is in accordance with the theory that most human blood vessels are only innervated by sympathetic vasoconstrictor fibers [16]. Furthermore, the nerves of plexuses around pulmonary arteries within the lung are exclusively innervated by postsynaptic sympathetic fibers [17].

PAH is a pulmonary vascular disease characterized by vasoconstriction and proliferative and obstructive remodeling of the pulmonary vessel wall [18-20]. Moreover, the remodeling process occurs in the distal pulmonary arteries [18]. Although the exact processes that initiate the pathological changes of PAH are still unclear, sympathetic activation may contribute to pulmonary arteriolar remodeling when the pulmonary vasculature is exposed to factors such as hypoxia, smoking and shear stress [1, 21]. The pulmonary circulation is richly innervated with sympathetic nerve endings derived from the cardiac plexuses, and anterior and posterior, pulmonary plexuses [15]. Norepinephrine release from sympathetic nerves stimulates α_1-adrenoreceptors on pulmonary vascular smooth muscle cells by two different mechanisms to cause contraction and proliferation [21]. Compared with the proximal segments, there was a slight decrease in the number of nerves in the distal segments. In addition, the majority of nerves were greater than 300 μm in diameter in the distal segments. One potential explanation for this anatomic variation is that the distal segments are mainly supplied by the pulmonary plexuses, which are formed by a combination of sympathetic trunks and the vagus nerve [22]. Pulmonary plexuses are divided into periarterial and peribronchial plexuses after entering the lung. Periarterial plexuses are almost solely formed by the postsynaptic sympathetic fibers, which innervate pulmonary vascular smooth muscle exclusively [17]. Vagus nerve innervates the branches of the bronchial tree [22]. Our data showed that the total number of nerves located in the posterior region of the bifurcation and the pulmonary trunk was greater than that in the anterior region; this anatomic distribution characteristic may be related to the cardiac plexus. This innervation is commonly described as lying on the anterior surface of the bifurcation of the trachea, as it is at the posterior aspect of the bifurcation of the pulmonary trunk [15], which aligns with our findings. Moreover, 68% of nerves were greater than 300 μm and 65.10% of nerves were greater than 500 μm, lying on the posterior region of the bifurcation and the pulmonary trunk, respectively. Our data showed that larger nerve bundles were located in the posterior region of the bifurcation and the pulmonary trunk. Due to the location of the cardiac plexus near the ostia of the bilateral pulmonary artery, the nerves of the proximal segment may be derived from the branches of the plex-

us. In addition, the pulmonary and cardiac plexuses are connected [15, 17, 22]. Therefore, a large number of fibers may be located in the proximal regions of both pulmonary arteries, supporting our findings.

The sympathetic nervous system is recognized as a target for the treatment of several disorders, including arrhythmias, resistant arterial hypertension, and idiopathic pulmonary hypertension [23]. Although PADN as a novel treatment for pulmonary hypertension is under investigation, peri-arterial pulmonary nerve distribution has not been elucidated previously. Our results indicate that the application of thermal energy could be focused on the proximal and distal segments, the posterior region of the bifurcation, and the pulmonary trunk (**Figure 7**). The present study may provide needed nerve distribution information for PADN.

There were some limitations to our study. First, the number of samples was limited (n=6); second, we only examined 4 to 5 mm of the peri-arterial tissue around the pulmonary artery; and third, the anatomic characteristics of pulmonary artery nerves in the canine model may not be sufficiently similar to those in humans. However, because this is the first study of the anatomic distribution of pulmonary arteries, valuable information can be retrieved from our findings.

Conclusions

In our study, we identified sympathetic fibers at a depth of 4 to 5 mm around the pulmonary lumen intima, with the greatest density of nerve endings located in the posterior region of the bifurcation and pulmonary trunk, as well as in the initial portions and roots of the right and left pulmonary arteries. The anatomic characteristics of the nerve distribution of pulmonary arteries may provide useful information for the development of efficient PADN.

Disclosure of conflict of interest

None.

Address correspondence to: Dr. Yuehui Yin, Department of Cardiology, Chongqing Cardiac Arrhythmias Therapeutic Service Center, The Second Affiliated Hospital of Chongqing Medical University, 76 Linjiang Road, Yuzhong District, Chongqing, 400010, China. Tel: (86) 135-0833-5502; Fax: 63693766; E-mail: yinyh63@163.com

References

[1] Sutendra G and Michelakis ED. Pulmonary arterial hypertension: challenges in translational research and a vision for change. Sci Transl Med 2013; 5: 208sr205.

[2] Michelakis ED, Wilkins MR and Rabinovitch M. Emerging concepts and translational priorities in pulmonary arterial hypertension. Circulation 2008; 118: 1486-1495.

[3] Tuder RM, Abman SH, Braun T, Capron F, Stevens T, Thistlethwaite PA and Haworth SG. Development and pathology of pulmonary hypertension. J Am Coll Cardiol 2009; 54: S3-9.

[4] Taniguchi Y, Emoto N, Miyagawa K, Nakayama K, Kinutani H, Tanaka H, Shinke T and Hirata K. Noninvasive and simple assessment of cardiac output and pulmonary vascular resistance with whole-body impedance cardiography is useful for monitoring patients with pulmonary hypertension. Circ J 2013; 77: 2383-2389.

[5] Humbert M, Morrell NW, Archer SL, Stenmark KR, MacLean MR, Lang IM, Christman BW, Weir EK, Eickelberg O, Voelkel NF and Rabinovitch M. Cellular and molecular pathobiology of pulmonary arterial hypertension. J Am Coll Cardiol 2004; 43: 13S-24S.

[6] Michelakis ED. Pulmonary arterial hypertension: yesterday, today, tomorrow. Circ Res 2014; 115: 109-114.

[7] Velez-Roa S, Ciarka A, Najem B, Vachiery JL, Naeije R and van de Borne P. Increased sympathetic nerve activity in pulmonary artery hypertension. Circulation 2004; 110: 1308-1312.

[8] Chen SL, Zhang FF, Xu J, Xie DJ, Zhou L, Nguyen T and Stone GW. Pulmonary artery denervation to treat pulmonary arterial hypertension: the single-center, prospective, first-in-man PADN-1 study (first-in-man pulmonary artery denervation for treatment of pulmonary artery hypertension). J Am Coll Cardiol 2013; 62: 1092-1100.

[9] Burgi K, Cavalleri MT, Alves AS, Britto LR, Antunes VR and Michelini LC. Tyrosine hydroxylase immunoreactivity as indicator of sympathetic activity: simultaneous evaluation in different tissues of hypertensive rats. Am J Physiol Regul Integr Comp Physiol 2011; 300: R264-271.

[10] Qin BZ, Li JS. The morthology and distribution of the cholinergic neuronal elements in the sacral and coccygeal spinal cord of the cat: an immunohistochemical study with monochonol

antibody to choline acetyltransferase. ACTA Anatomica Sinica 1988; 19: 368-374.
[11] Lee MK, Xu Z, Wong PC and Cleveland DW. Neurofilaments are obligate heteropolymers in vivo. J Cell Biol 1993; 122: 1337-1350.
[12] Ciarka A, Vachiery JL, Houssiere A, Gujic M, Stoupel E, Velez-Roa S, Naeije R and van de Borne P. Atrial septostomy decreases sympathetic overactivity in pulmonary arterial hypertension. Chest 2007; 131: 1831-1837.
[13] Ciarka A, Doan V, Velez-Roa S, Naeije R and van de Borne P. Prognostic significance of sympathetic nervous system activation in pulmonary arterial hypertension. Am J Respir Crit Care Med 2010; 181: 1269-1275.
[14] de Man FS, Handoko ML, van Ballegoij JJ, Schalij I, Bogaards SJ, Postmus PE, van der Velden J, Westerhof N, Paulus WJ and Vonk-Noordegraaf A. Bisoprolol delays progression towards right heart failure in experimental pulmonary hypertension. Circ Heart Fail 2012; 5: 97-105.
[15] Moore KL, Dalley AF, Agur AMR. Clinical Oriented Anatomy. In: Moore KL, editors. Thorax. 6th ed. Philadelphia: Lippincott Williams and Wilkins; 2010. pp. 58-119.
[16] Zhu DN, Wu BW, Fan XL. PHYSIOLOGY. Beijing, China: People's Medical Publishing House; 2008.
[17] Liu ZJ, Chen EY. Clinical anatomy books-the parts of chest and spin. Beijing, China: People's Medical Publishing House; 1994.
[18] Galiè N, Hoeper MM, Humbert M, Torbicki A, Vachiery JL, Barbera JA, Beghetti M, Corris P, Gaine S, Gibbs JS, Gomez-Sanchez MA, Jondeau G, Klepetko W, Opitz C, Peacock A, Rubin L, Zellweger M, Simonneau G; ESC Committee for Practice Guidelines (CPG). Guidelines for the diagnosis and treatment of pulmonary hypertension: the Task Force for the Diagnosis and Treatment of Pulmonary Hypertension of the European Society of Cardiology (ESC) and the European Respiratory Society (ERS), endorsed by the International Society of Heart and Lung Transplantation (ISHLT). Eur Heart J 2009; 30: 2493-2537.
[19] Ghofrani HA, Barst RJ, Benza RL, Champion HC, Fagan KA, Grimminger F, Humbert M, Simonneau G, Stewart DJ, Ventura C and Rubin LJ. Future perspectives for the treatment of pulmonary arterial hypertension. J Am Coll Cardiol 2009; 54: S108-117.
[20] Zhou S, Li M, Zeng D, Sun G, Zhou J and Wang R. Effects of basic fibroblast growth factor and cyclin D1 on cigarette smoke-induced pulmonary vascular remodeling in rats. Exp Ther Med 2015; 9: 33-38.
[21] Salvi SS. Alpha1-adrenergic hypothesis for pulmonary hypertension. Chest 1999; 115: 1708-1719.
[22] Sun SQ, Zhang SX. The human body of general morphology experiment. Beijing, China: Science Press; 2009.
[23] Stefanadis C. Arterial denervation: clinical implications and future perspectives. Hellenic J Cardiol 2013; 54: 339-340.